International Journal of Earth Sciences (2024) 113:1197–1211
https://doi.org/10.1007/s00531-024-02429-3

ORIGINAL PAPER

Xenoliths of the bode dike system: evidence for early Devonian arc-type magmatism and late Carboniferous–Permian crust reworking beneath the eastern Harz Mountains (Germany)

Armin Zeh[1] · Carl-Heinz Friedel[2] · Olaf Tietz[3] · István Dunkl[4]

Received: 5 December 2023 / Accepted: 17 May 2024 / Published online: 11 June 2024

Abstract
Xenoliths recovered from the post-Variscan Bode dike system of the eastern Harz Mountains provide evidence for the existence of an Early Devonian magmatic arc system hidden beneath very low-grade metasedimentary rocks of the Rhenohercynian Zone, but also for Late Carboniferous–Early Permian crust reworking. This interpretation is based on petrographic observations and whole-rock geochemical analyses of granite xenoliths, in addition to results of zircon U–Pb dating and Hf isotope analyses. Zircon grains recovered from variably deformed granite xenoliths yield ages between 419 and 393 Ma, interpreted to reflect the timing of granite intrusion. Rare zircon xenocrysts of Archean (ca. 2.92–2.65 Ga) and Proterozoic age (ca. 1.5 to 0.56 Ga), all with subchondritic $\varepsilon Hf_{420\ Ma}$ values (− 0.8 to − 5.5) indicate reworking of older crust. Compilation of age-Hf isotope data further suggests that the pre-Variscan granitoids beneath the Harz Mountains belong to the same magmatic arc system exposed widespread in the adjacent Mid-German Crystalline Zone, and interpreted to result from NW-ward subduction of the Rheic Ocean beneath Avalonia-Baltica. Zircon in xenoliths with granophyric texture yields ages at 400 Ma and 295–310 Ma, indicating re-melting of Devonian granitoid basement during post-Variscan rift-related magmatism, immediately prior to Bode dike intrusion.

Keywords Harz · Granite xenoliths · Zircon · U–Pb dating · Hf isotopes

Introduction

Presently, very little is known about the lower crust of the Harz Mountains forming part of the Rhenohercynian Zone of the Variscan Orogen after Kossmat (1927; Fig. 1a). The Variscan basement of the Harz Mountains mainly consists of very low-grade Paleozoic metasedimentary rocks, which were predominately deposited between the Early Devonian and Early Carboniferous in marine settings from different sources (Wachendorf et al. 1995; Huckriede et al. 2004; Schwab and Hüneke 2008; Schwab and Ehling 2008; Linnemann et al. 2023), and intensely folded during the Variscan orogeny at < 330 Ma (Schwab 2008, and references therein). High-grade metamorphic rocks are exposed only in the Ecker Gneiss complex (Fig. 1b), which was long considered to represent an exhumed sliver of Cadomian basement beneath the Harz Mountains. This interpretation, however, has been disproved by Geisler et al. (2005) and more recently by Linnemann et al. (2023), showing that the protoliths of metasedimentary rocks of the Ecker Gneiss complex were supplied from Baltica, and deposited during the Devonian at < 410 Ma (410 ± 10; 414 ± 6; 406 ± 12 Ma: U–Pb ages of the youngest detrital zircon grains from three samples). Subsequently, during the Variscan orogeny, the Ecker Gneiss complex was affected by a granulite-facies metamorphic overprint (Appel et al. 2019).

During the Late Carboniferous to Early Permian, the Paleozoic rock units of the Harz Mountains were intruded

✉ Armin Zeh
armin.zeh@kit.edu

[1] Institute for Applied Geoscience, Mineralogy and Petrology, KIT-Karlsruhe Institute of Technology, Adenauerring 20b, Geb. 50.4, 76131 Karlsruhe, Germany

[2] Karl-Marx-Str, 56, 04158 Leipzig, Germany

[3] Senckenberg Museum for Natural History Görlitz, Am Museum 1, 02826 Görlitz, Germany

[4] Geoscience Center, Department of Sedimentology & Environmental Geology, Georg-August-University Göttingen, Goldschmidtstrasse 3, 37077 Göttingen, Germany

by mafic and felsic plutonic rocks, comprising the Harzburg gabbro, the Oker, Brocken and Ramberg granites at ca. 300 Ma (Baumann et al. 1991; Goll et al. 1998; Linnemann et al. 2023), but also by N–S, NW–SE and E–W trending dikes of similar age (Fig. 1b). In the northeastern Harz Mountains, low-grade sedimentary rocks of Devonian age, the Wissenbach slates, were intruded by E–W trending, steep dipping dikes of the Bode dike system, prior to emplacement of the Ramberg pluton, as indicated by field relationships (Schust 1958). This dike system is made up by a variety of subvolcanic rocks comprising kersantite, fine-grained granite porphyry, microgranodiorite and microgranite (Tietz 1995, 1996), and locally contains abundant xenoliths up to metre size, comprising metamorphic rocks and granitoids. Presently, nothing is known about the composition of the granitoid rocks, their geotectonic setting and intrusion ages, i.e. whether the granitoid protoliths intruded during the pre-, syn- or post-Variscan evolution. In this context, we note that pre-Variscan and Variscan granitoids are nowhere exposed within the Rhenohercynian realm of Germany, neither in the Harz Mountains nor in the Rhenish Massif (Fig. 1a). In this study, we present the first set of data of granite xenoliths from the Bode dike system, comprising petrographic observations, whole-rock geochemical data, results of zircon U–Pb dating and Hf isotope analyses. These data in combination will provide new information about the composition, origin and evolution of the deeper crust of the eastern Harz Mountains. By comparison with data from adjacent geological units, these will also place new constraints on the pre- and post-Variscan evolution in Central Europe.

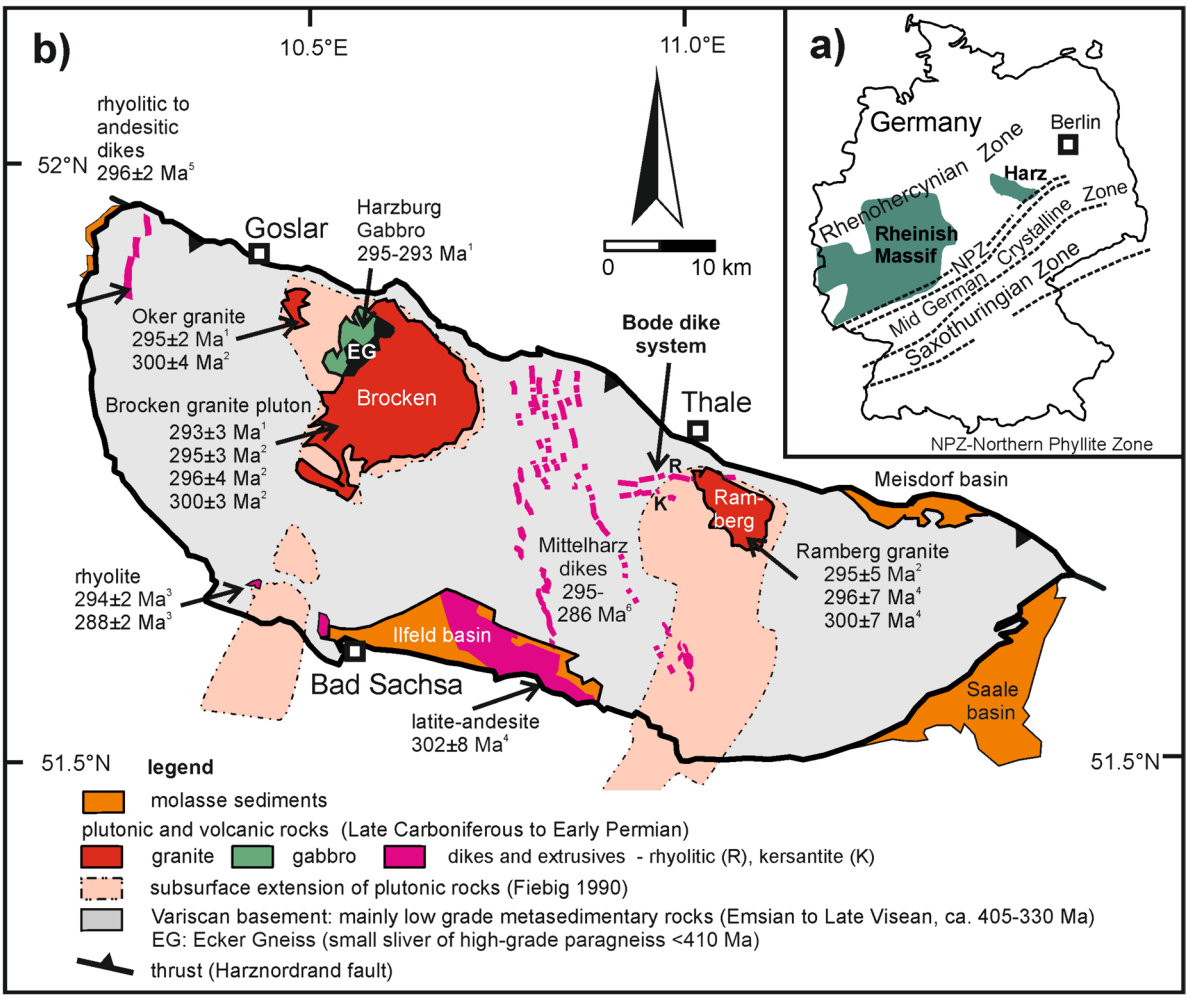

Fig. 1 **a** Position of the Harz Mountains in Germany. **b** Simplified geological map of the Harz Mountains with geochronological data of plutonic and volcanic rocks. Geochronological data: (1) U–Pb zircon (Baumann et al. 1991), (2) U–Pb zircon (Linnemann et al. 2023), (3) Ar–Ar of biotite and sanidine (Lippolt and Hess 1996), (4) K–Ar of biotite and muscovite (Goll et al. 1998), (5) Ar–Ar whole rock (Goll in von Seckendorff 2012), (6) Pb–Pb zircon (Obst et al. 2001)

Geological setting

The Bode dike system is exposed in the northeastern part of then Harz Mountains, close to the city of Thale, mostly west of the Ramberg pluton (Fig. 1b). It comprises two subparallel E–W trending dikes, a southern branch made up by the kersantite of Treseburg, and a northern branch dominated by granite porphyry (Figs. 1, 2). The northern branch, our study area, is well exposed along the northern slope of the Bode stream valley (Fig. 2), where it transects Wissenbach slate of middle Devonian age (Eifelian), intercalated by numerous diabase sills and dikes.

The northern branch is 3–8 m wide, about 12 km long, and hosts several stages of magma injections (Fig. 2). The first stage is reflected by a dense zone of fine-grained granite porphyry, which is free of xenoliths and commonly forms the margin of the dike, both hanging and footwall against the surrounding Wissenbach slates. Subsequently, the same dike was injected in its centre part by melts of dacitic and rhyolitic composition, both rich in xenoliths (Tietz 1995, 1996). In the field, both phases show a microgranitic structure, and can be distinguished from each other by their different colours, with the granodioritic phase showing a dark, and the microgranitic phase a bright colour. Sharp and gradational contacts between microgranite and microdiorite suggest a fast sequence of injection, and locally point to magma mingling either within the dike and/or immediately prior to magma injection (Tietz 1995, 1996). Composite dikes, as described above, only occur in the area west of the Ramberg pluton over a length of almost 600 m, and microgranitic and microgranodioritic varieties with xenoliths just over 350 m along strike along the northern slope of the Bode stream valley, north of the cliff "Blaue Klippe" (Fig. 2).

Presently, no radiometric ages are available for the Bode dike system. Field relationships indicate that it is younger than the surrounding Wissenbach slates (Eifelian) and older than the Ramberg pluton (Schust 1958; Fig. 1b). The age of the Ramberg pluton is constrained by results of K–Ar dating of biotite (296 ± 7 Ma) and K-feldspar (300 ± 7 Ma) presented by Goll et al. (1998), and a recently published U–Pb zircon age of 295 ± 5 Ma (LA-ICP-MS; Linnemann et al. 2023). We note that all these ages are significantly older than a zircon U–Pb age of 283 ± 3 Ma (also LA-ICP-MS), previously presented by Zech et al. (2010).

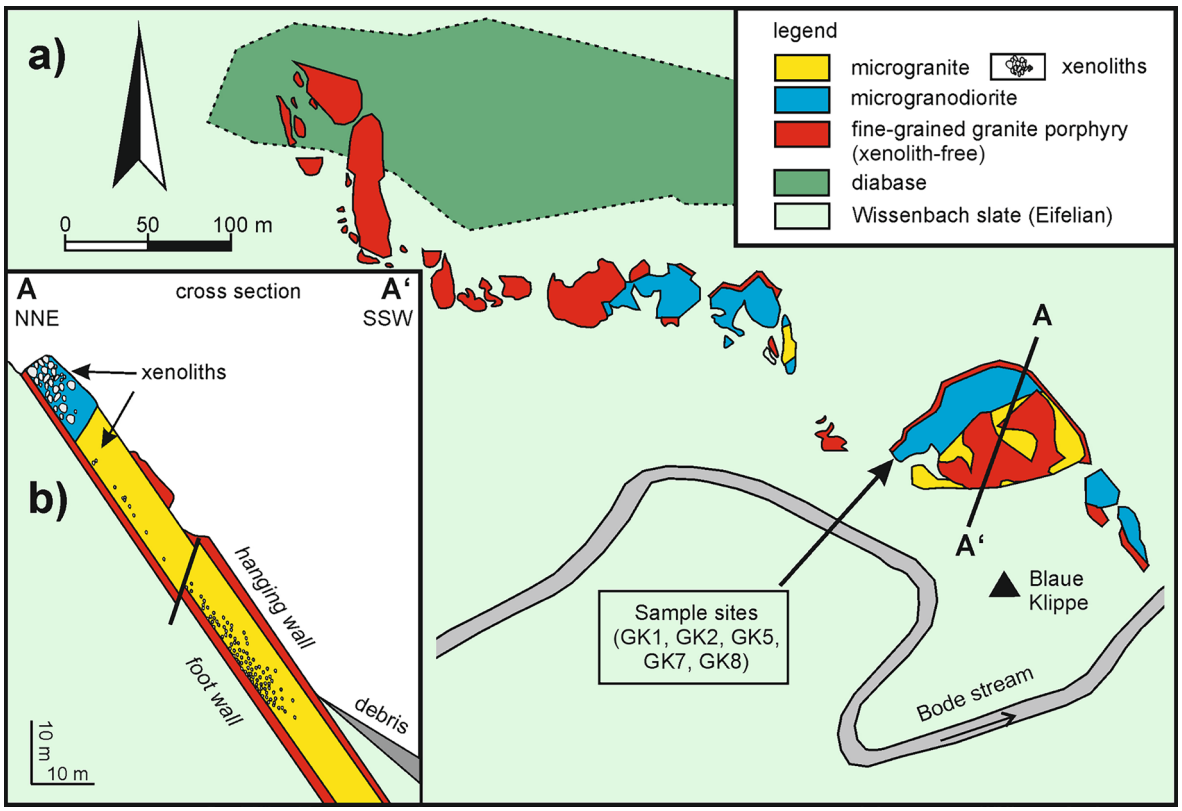

Fig. 2 Field relationships of the composite northern Bode dike in the Bode stream valley. **a** Geologic map with sample sites, and **b** cross section (modified after Tietz 1996). The Bode dike system results from three phases of magma injection: (1) margins made up of granite porphyry, (2) microgranodiorite, and (3) microgranite

The xenolith suite included in the microgranite and microdiorite varieties of the northern Bode dike comprises metasedimentary rocks, dioritoids (autoliths), amphibolites, paragneisses, micaschists and granitic rocks (Tietz 1996; this study). Leucogranite xenoliths up to cubic metre in size occur abundantly in the microgranodioritic intrusion (Figs. 2 and 3).

Sample description

The granite xenoliths investigated in this study were all sampled from the microgranodioritic variety of the Bode dike exposed in several cliffs along the northern slope of the Bode stream valley (Fig. 2). The granitoids are mostly leucocratic, and affected by a different degree of ductile and brittle deformation, showing all transitions from non-deformed granite to orthogneiss (Figs. 3, 4). Based on thin section observations, two types of granite can be distinguished: (1) granitoids with ductile deformation features (samples GK1, GK7, GK8), and (2) undeformed granites with granophyric textures (samples GK2 and GK5; Fig. 4). The granitoids are medium- to course-grained, commonly show a foliation (more or less pronounced) and distinct mylonitic textures, reflected by dynamically recrystallized quartz ribbons surrounding feldspar-rich domains dominated by perthitic K-feldspar and minor plagioclase (Fig. 4a, b). Samples with granophyric textures (GK2 and GK5) are characterised by euhedral quartz phenocrystals, surrounded by a relatively fined-grained matrix dominated by granophyric K-feldspar-quartz intergrowths, locally surrounding plagioclase phenocrystals (Fig. 4c, d).

Analytical techniques

U–Pb dating and zircon imaging

Zircon grains were recovered from five granite xenoliths (GK1, GK2, GK5, GK7, GK8). Sample GK1 was processed and analysed at University Göttingen (UG), and the other four samples at Karlsruhe Institute of Technology (KIT). The samples were crushed with Jaw crusher and steel disc mill to grain sizes < 500 µm, and the heavy mineral fraction enriched by panning (only at KIT) or by heavy liquids and magnetic separation at UG. Finally, zircon grains were manually picked from concentrates under ethanol, mounted on double-sided tape. At KIT, the zircon grains were sputtered with Au for 10 s, and imaged for their morphologies by back-scattered electron (BSE) microscopy using a TESCAN VEGA2 scanning electron microscope (at the Department of Petrology). Representative zircon images are shown in Fig. 5. Subsequently, the same grains were mounted with epoxy and grinded to expose their centre parts (also done at UG). The polished grains were imaged again by BSE at KIT, and CL (cathodoluminescence) at UG, to get information about their internal zoning (Fig. 5 and ESM—electronic supplement material). Based on these images, the most pristine zircon grains/domains were selected for *in situ* U–Pb dating and Hf isotope analyses.

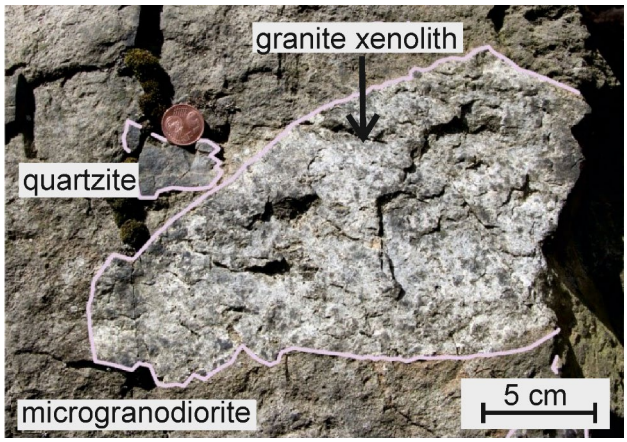

Fig. 3 Field relationships of xenoliths in the Bode dike. Coarse-grained granite xenolith of ca. 25 cm size, and small quartzite xenolith in a grey microgranodioritic matrix

Uranium–Pb analyses were performed by laser ablation–sector field–inductively coupled plasma–mass spectrometry (LA-SF-ICP-MS) at UG and KIT. Detailed information about analytical conditions in each lab is presented in ESM (Table S1). In each lab, zircon grains of unknown age were analysed together with reference zircon (for details see ESM: Table S2). At KIT, all raw data were corrected offline using an in-house MS Excel© spreadsheet program (Gerdes and Zeh 2006, 2009). A common Pb correction based on the interference and background-corrected ^{204}Pb signal, and a model Pb composition were applied (Stacey and Kramers 1975). At UG, data processing was carried out with the software URANOS of Dunkl et al. (2008). The results of measurements of unknowns and reference zircon grains are presented in ESM (Table S2). Concordia diagrams were plotted by means of the software ISOPLOT 3.75 (Ludwig 2012).

Hf isotope analyses

Lutetium-Hf isotope analysis was carried out with a Resolution M-50 193 nm ArF Excimer laser system coupled to a Thermo Scientific multicollector (MC)-SF-ICP-MS (Neptune Plus) at FIERCE Frankfurt am Main, Germany. The analytical protocols used are the same as described in detail by Gerdes and Zeh (2006), and Zeh and Gerdes

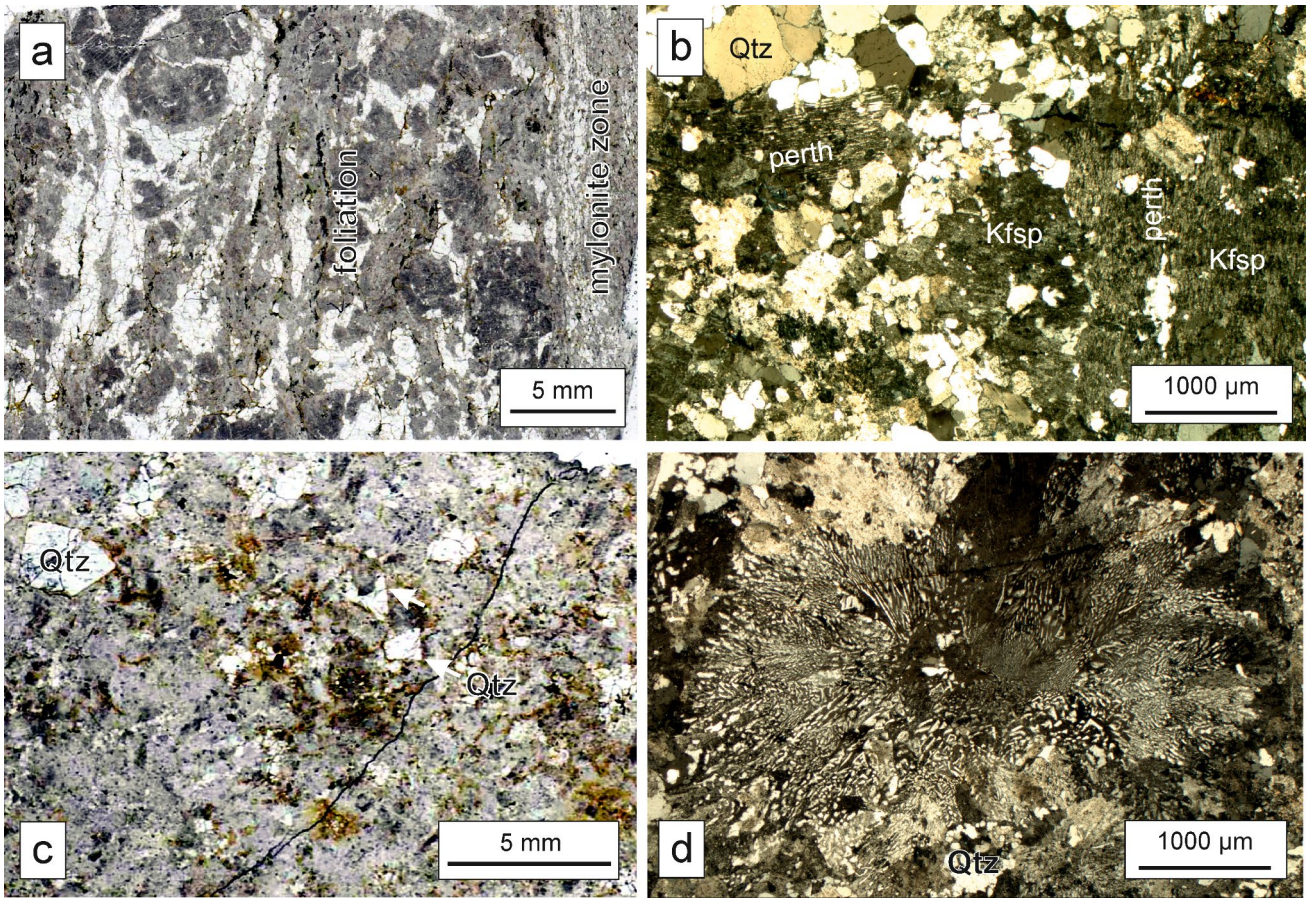

Fig. 4 Scans and photomicrographs (crossed nicols) of granite xenoliths with different structures from the Bode dike: **a**, **b** deformed granitoid, sample GK7; **c**, **d** granophyric granite, sample GK5. **a**, **b** Sample GK7 is a leucocratic, well-foliated granite gneiss, transect by mylonite zones with dynamically recrystallized quartz. It mainly consists of quartz (Qtz) and perthitic K-feldspar (perth Kfsp), (c, d) Sample GK-7 contains euhedral quartz phenocrystals (Qtz) within a fine-grained matrix dominated by K-feldspar-quartz granophyric intergrowths

(2012; and reference therein). Detailed operating conditions for Lu–Hf isotope analyses and results of standard measurements are presented in ESM (Tables S1 and S3). Multiple measurements of reference zircon GJ1 and Temora-1 during the analytical session yielded $^{176}Hf/^{177}Hf$ ratios of 0.2820002 ± 0.000022 (2σ S.D.), and 0.282701 ± 0.000046 (2σ S.D.) respectively, in agreement with published values (Woodhead and Hergt 2005). For calculation of the epsilon Hf (εHf_t), the chondritic uniform reservoir (CHUR) was used as recommend by Bouvier et al. (2008); $^{176}Lu/^{177}Hf$ and $^{176}Hf/^{177}Hf$ of 0.0336 and 0.282785, respectively, and a decay constant of 1.867×10^{-11} (Scherer et al. 2001; Söderlund et al. 2004). All two-stage Hf model ages (T_{DM}) were calculated by applying $^{176}Hf/^{177}Hf = 0.283181 \pm 0.00023$ ($n = 46$) and $^{176}Lu/^{177}Hf = 0.038055$ for the depleted mantle (DM) evolutionary line (average MORB composition of Atlantic and Indian Oceans of Chauvel and Blichert-Toft 2001), resulting in a depleted mantle (DM) evolutionary line ranging from + 14 (today) to zero (at 4.56 Ga). Crustal evolutionary trends were modelled by applying $^{176}Lu/^{177}Hf = 0.0113$ for continental crust (average of Taylor and McLennan 1985, and Wedepohl 1995). For all zircon xenocrysts, initial $^{176}Hf/^{177}Hf$, εHf_t and T_{DM} were calculated using the $^{207}Pb/^{206}Pb$ ages obtained for the respective zircon domains (ESM: Table S2).

Whole-rock geochemical analyses

Whole-rock geochemical analyses were carried out on powders obtained by jaw crushing and Achate disc milling from 4 granite samples. For analysis, 0.5 g sample powder was mixed with 5 g SPECTROMELT A 12 (66% di-lithium tetraborate/34% lithium metaborate) and fused at a burner station. Major and minor element analyses on fusion discs

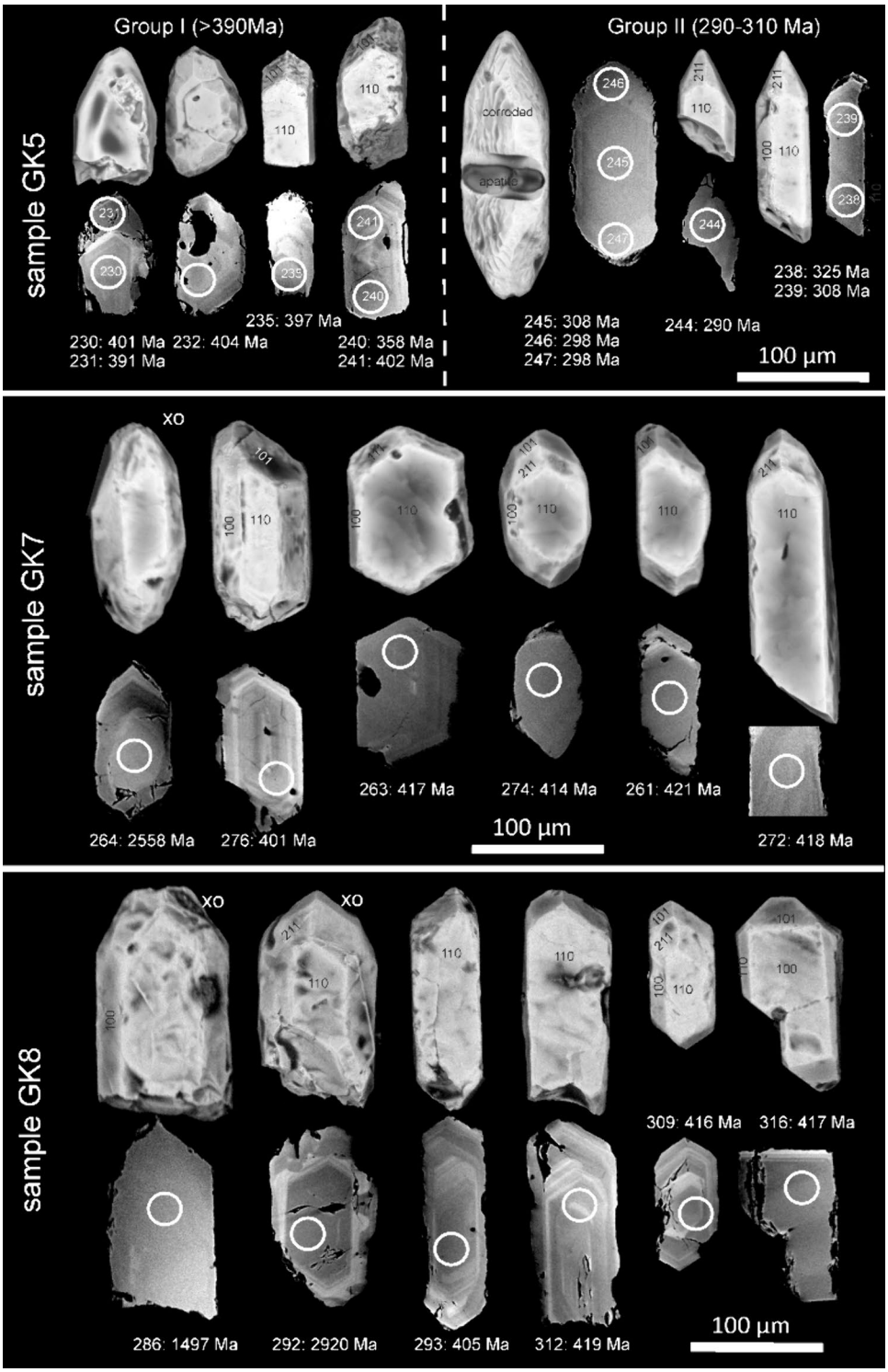

Fig. 5 Back-scattered electron images of zircon grains found in granophyric granite (sample GK5), and granitoids (samples GK7 and GK8). Images show zircon morphologies (numbers 100, 111, 211 etc. represent face indices), and internal structures (images with circles, representing laser spot positions), xo-xenocryst zircon. Numbers beneath zircon images represent no. of analyses and $^{206}Pb/^{238}U$ age. Note that in sample GK5, two groups of zircon can be distinguished, based on typologies and ages (for details see text)

were obtained using a Bruker S4 Explorer wavelength-dispersive X-ray fluorescence (XRF) spectrometer at the Laboratory for Environmental and Raw Materials Analysis (LERA), Institute of Applied Geosciences at KIT, Germany. Matrix effects were corrected automatically by the Bruker software. The relative analytical error for major and minor elements is 1% and 1–8%, respectively. Volatile components are reported as loss of ignition (LOI).

Trace elements were analysed subsequently by LA-SF-ICP-MS (193nm ArF Excimer laser, Analyte Excite +, Teledyne Photon Machines) coupled to a Thermo Scientific Element XR instrument at KIT, on the same fusion discs used

for the WDXRF analyses. The fusion discs were measured together with reference glasses NIST-SRM612 (primary standard), BIR1, BHVO2 and BCR2G (secondary standards). On each fusion disc, five spots were measured with a diameter of 85 µm alternating with measurements of reference material. The analyses were obtained with Al-H cones using the following instrument parameters (for standards and fusion discs): ablation duration = 25 s on peak after 20 s background measurement, laser repetition rate = 10 Hz, laser fluence = 7 J/cm^2; mixed Ar–He–N_2 carrier gas (Ar = 0.77 L/min, He cell gas = 0.30 L/min, He cup gas = 0.22 L/min, N_2 = 12 mL/min), RF power = 1125 W. The oxide formation rate monitored as $^{254}UO_2/^{238}U$ was < 0.08% during the analytical session. Raw data were processed by means of the software GLITTER (van Achterberg 2000), using SiO_2 as an internal standard. The geochemical data of unknown rock samples and reference materials are presented in ESM (Table S4). Values represent the mean of five in situ fusion disc analyses. The errors are commonly < 2% (1σ mean) for most trace elements with concentrations > 1 µg/g.

Results

Geochemical data

Whole-rock geochemical data were obtained from four granite xenoliths (granophyric granite: GK2, GK5; granitoids: GK7, GK8). The results are shown in Figs. 6 and 7. All analysed granites show high silica (SiO_2 = 72.5 to 75.1 wt%) and alkali oxide contents ($Na_2O + K_2O$ = 4.2 to 8.7 wt%). Based on major element composition, the granites are classified as peraluminous to subaluminous, magnesian and calc-alkalic (GK7, GK8) or alkali-calcic (GK2, GK5) in composition (Fig. 6a–c). The trace element patterns of all samples normalised to primitive mantle are similar, and characterised by relative depletion in Ba, Nb, Ti, Sr and P, and enrichment in Pb, ± U and Th (Fig. 6e). The chondrite-normalised REE patterns are also similar. They reveal negative europium anomalies (Eu/Eu^*_N = 0.27–0.5), enrichment of LREE over HREE [$(La/Yb)_N$ = 7.1–13.2] and a moderate fractionation of HREE [$(Gd/Yb)_N$ = 1.4–2.3]. In discrimination diagrams for geotectonic setting, all samples plot in the field for volcanic arc granites (Fig. 7a, b).

Results of zircon U–Pb dating

Zircon grains from five xenoliths could be recovered for U–Pb dating, mostly more than 50 grains per sample, but only 5 grains from sample GK2 (granophyric granite). These five grains gave late Permian to Mesozoic $^{206}Pb/^{238}U$ ages < 261 Ma (ESM: Table S2), and some analyses show a high degree of discordance (e.g. grain U228), suggesting significant Pb loss after zircon growth. In contrast, zircon grains of the granitoid samples GK7 and GK8 yield concordia ages of 418.9 ± 1.8 Ma (n = 17 out of 27), and 417.7 ± 1.8 Ma (n = 16 out of 25), respectively (Fig. 8; Table 1), which are interpreted to date the time of magma crystallisation; also supported by oscillatory zircon zoning patterns (Fig. 5) and zircon Th/U ratios between 0.2 and 1.4 (ESM: Table S2). In situ U–Pb analyses of magmatic zircon grains/domains of granitoid sample GK1 reveal a relatively wide scatter in $^{206}Pb/^{238}U$ ages between 416 ± 6 and 368 ± 5 Ma. Assuming a coherent magmatic population, nine out of the 20 analyses provide a mean $^{206}Pb/^{238}U$ ages of 393 + 4.8/− 1.7 Ma (calculated by "T*uff*ZircAge" algorithm of Ludwig and Mundil 2002; Fig. 8b). A few zircon analyses from the three granitoid samples gave significantly older $^{207}Pb/^{206}Pb$ ages, ranging from 1451 to 559 Ma in sample GK1, 2652 to 1401 Ma in sample GK7, and from 2920 to 1497 Ma in sample GK8. These grains represent xenocrysts and indicate involvement of older crustal matter of Archean to Proterozoic age during granite formation.

Sample GK5 (granophyric granite) contains a complex zircon population, which can be subdivided in two major groups, based on U–Pb ages and zircon morphologies (Figs. 5 and 8e). Group I comprises euhedral zircon grains dominated by {101} pyramids, which yield Devonian $^{206}Pb/^{238}U$ ages ranging from 404 ± 6 to 391 ± 7 Ma (similar to zircon ages obtained from the granitoid samples GK7 and GK8; Fig. 8c, d). The three oldest analyses give a concordia age of 402.4 ± 3.6 Ma. The youngest age of 391 ± 7 Ma was obtained from a rim (spots 230 and 231; see Fig. 5), perhaps formed during a somewhat younger magmatic event. At least some of the Devonian zircon grains/domains were affected by serious Pb loss, as indicated by significant differences in $^{206}Pb/^{238}U$ ages obtained by double analyses of the same zircon zone (e.g. spots 240 and 241 in Fig. 5). Group II zircon grains are dominated by {211} pyramids (more or less corroded), and reveal Late Carboniferous to Early Permian ages (Figs.5 and 8e). The most reliable U–Pb analyses, i.e. from grains with a high degree of concordance (90–100%) yield $^{206}Pb/^{238}U$ ages between 308 ± 5 and 285 ± 4 Ma (n = 8). Five of these analyses give a concordia age of 296.4 ± 2.3 Ma, which is interpreted to represent magma crystallisation. Ages between c. 390 and c. 296 Ma perhaps result from a creeping, differential Pb loss, which affected the Devonian zircon population during Early Permian magmatism. In summary, combined information from zircon images and U–Pb ages suggests that the granophyric granite GK5 emplaced and crystallised during the Late Carboniferous–Early Permian, and that the parental magma was formed by the re-melting of Devonian granite basement (for more discussion see chapter 5.1: "Crustal evolution beneath the Harz Mountains").

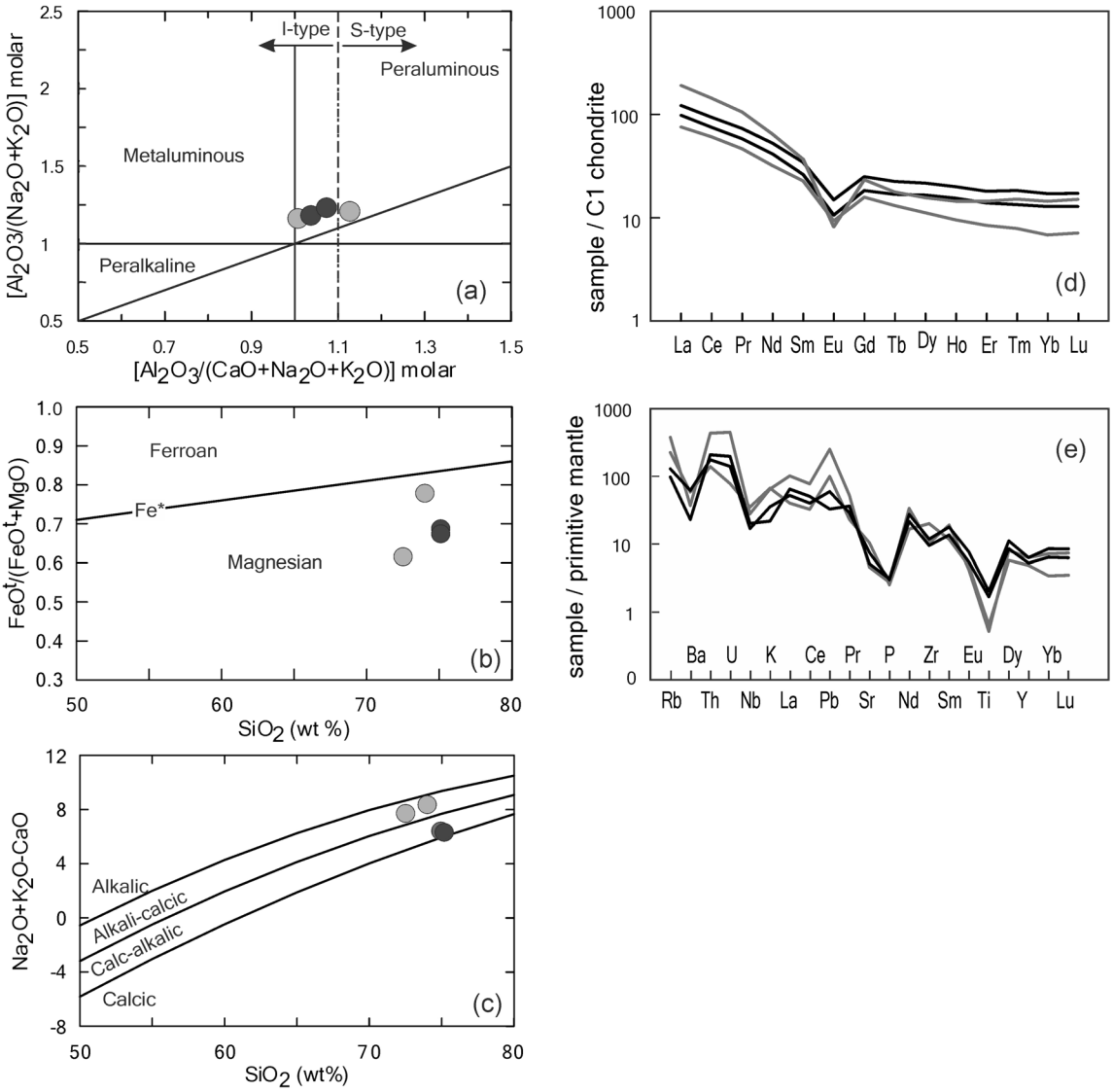

Fig. 6 Various classification diagrams for granites based on **a**–**c** major elements, **d**–**e** trace elements (black dots: granitoids GK7, GK8, grey dots: granophyric granites GK2, GK5). **a** Shand index plot with discrimination fields after Maniar and Piccoli (1989). The dividing line between I- and S-type granites is after Chappell and White (1974). **b** $FeO^t/(FeO^t+MgO)$ versus SiO_2 (wt%) classification diagram (Frost et al. 2001). The Fe-number (Fe*) dividing line is after Frost and Frost (2008). **c** Modified alkali-lime index (Na_2O+K_2O–CaO in wt%) versus SiO_2 (wt%) classification diagram (Frost et al. 2001). **d** Rare-earth element patterns of granites normalised to C1 chondrite after McDonough and Sun (1995). **e** Trace element composition of granites normalised to primitive mantle after McDonough and Sun (1995)

Results of Hf isotope analyses

Hafnium isotope compositions were measured on zircon grains of three samples, granophyre granite GK5, and the granitoids GK7 and GK8. Magmatic zircon grains of all three samples show overlapping $^{176}Hf/^{177}Hf_t$ ratios (Table 1). These range from 0.282439 ± 0.000043 (sample GK5–group I) to 0.282455 ± 0.000067 (sample GK7), and correspond to εHf_{410Ma} between -2.4 ± 2.7 and -3.3 ± 1.4 (or $\varepsilon Hf_{295Ma} = -5.0 \pm 1.2$), and two-stage Hf model ages between 1.25 ± 0.14 Ga and 1.30 ± 0.06 Ga (all errors are 2 sigma)—(Fig. 9; ESM- Table S3). Significantly lower $^{176}Hf/^{177}Hf_t$ ratios between 0.280909 and 0.281935 were only obtained from zircon xenocrysts, corresponding to Hf model ages between 2.17 and 3.29 Ga (ESM).

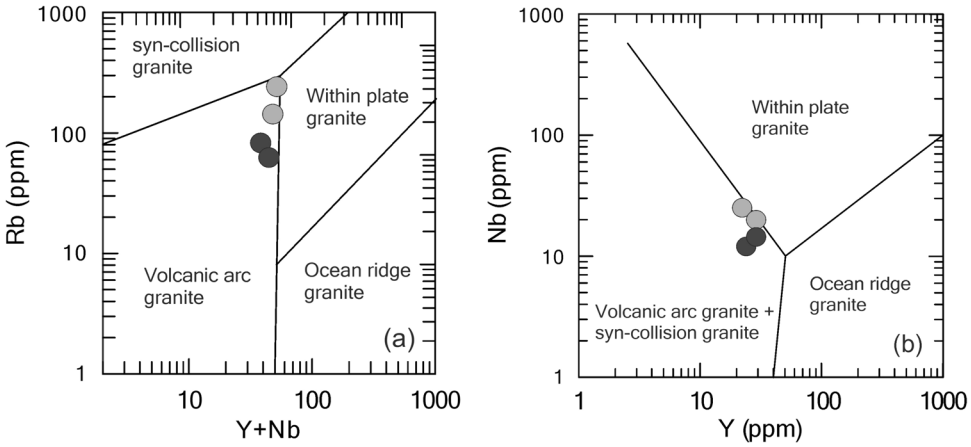

Fig. 7 Discrimination diagrams **a** Rb-(Y + Nb) and **b** Nb-Y for granites after Pearce et al. (1984). (black dots: granitoid samples GK7, GK8; grey dots: granophyric granites GK2, GK5)

Discussion

Crustal evolution beneath the Harz Mountains

Results of zircon U–Pb dating of xenoliths from the Bode dike reveal that the basement of the eastern Harz Mountains, hidden beneath very low-grade sedimentary rocks of middle Devonian age, hosts granitic rocks, which were formed during two stages of magmatic evolution (Table 1). Older granites, affected by a different degree of ductile deformation, emplaced and crystallised during the Early Devonian between 419 and 393 Ma, and younger granites with granophyric textures at ca. 295 Ma during the Late Carboniferous–Early Permian.

Combined results of whole-rock geochemistry and zircon U–Pb–Hf isotope analyses suggest that the magmatic protoliths of the granitoids intruded into a supra-subduction zone (magmatic arc) setting, and underwent assimilation and fractionation during emplacement within the crust. This interpretation is backed by the mildly peraluminous, calc-alkaline character, highly fractionated REE patterns with negative Eu-anomalies (pointing to fractionation in the stability field of plagioclase in relative shallow magma chambers), negative Nb–Sr–Ti and positive Pb anomalies in primitive mantle normalised diagrams (Fig. 6), and by discrimination diagrams for geotectonic setting (Fig. 7). Assimilation of older crust is indicated by zircon xenocrysts with $^{207}Pb/^{206}Pb$ ages between 2920 and 559 Ma found in three xenoliths (Fig. 5, ESM Table S3), and reworking of older crust by subchondritic εHf_{400Ma} values between − 0.8 and − 4.6. These values could result either from mantle-wedge enrichment by "sediments" during previous subduction (e.g. Laurent and Zeh 2015; Couzinie et al. 2016, and references therein), and/or from assimilation of crustal rocks during magma ascent. Two-stage Hf model ages indicate that the reworked crust was derived from a depleted mantle source at ca. 1.2 Ga, on average (Fig. 9). Finally, we note that zircon grains of the samples GK7 and GK8 show a predominance of {110} over {100} faces (Fig. 5), suggesting crystallisation at relatively low temperatures, mostly < 700 °C according to the classification scheme of Pupin (1980). These temperatures are slightly lower than zircon-in-melt saturation temperatures of 759 to 771 °C, based on whole-rock compositions of the investigated samples and the calibration of Harrison and Watson (1983).

The granophyric granite GK5 crystallised at 296.4 ± 2.3 Ma, which is suggested by a concordia age obtained from 5 grains of group II zircon dominated by {211} pyramids (Table 1, Figs. 5 and 8). This age reflects magma crystallisation during the Late Carboniferous–Early Permian, and overlaps within analytical error with an U–Pb zircon age of 295.0 ± 4.5 Ma, recently presented for the Ramberg pluton by Linnemann et al. (2023). This overlap and field relationships indicate that the Bode dike system formed immediately prior to Ramberg pluton emplacement. Zircon grains recovered from the granophyre sample GK2 yields late Permian to Triassic $^{206}Pb/^{238}U$ ages < 260 Ma. These ages are geologically meaningless, and most likely result from Pb loss. The finding of both Devonian and Permian zircon grains in sample GK5 further suggests that the granophyric granites result from partial melting of Devonian granites at depth during Late Carboniferous–Early Permian heating. This interpretation is also backed by similar normalised trace element patterns (Fig. 6) and overlapping Hf isotope compositions (Table 1, Fig. 9). Partial crust melting was most likely caused by mantle upwelling related to crust extension (Fig. 10), which affected wide parts of Central Europe during the Late Carboniferous–Early Permian (e.g.Ziegler 1990; van Wees et al. 2000; Wilson et al. 2004; McCann et al. 2006 and references therein). We note that the age obtained for the granophyric granite xenoliths overlaps intrusion ages derived for granites, gabbros, and intermediate to felsic dikes of the Harz Mountains (Fig. 1), and for diorites, granites and volcanic rocks of the Thuringian Forest (Zeh and Brätz 2000; Zeh et al. 2000; Lützner et al. 2021).

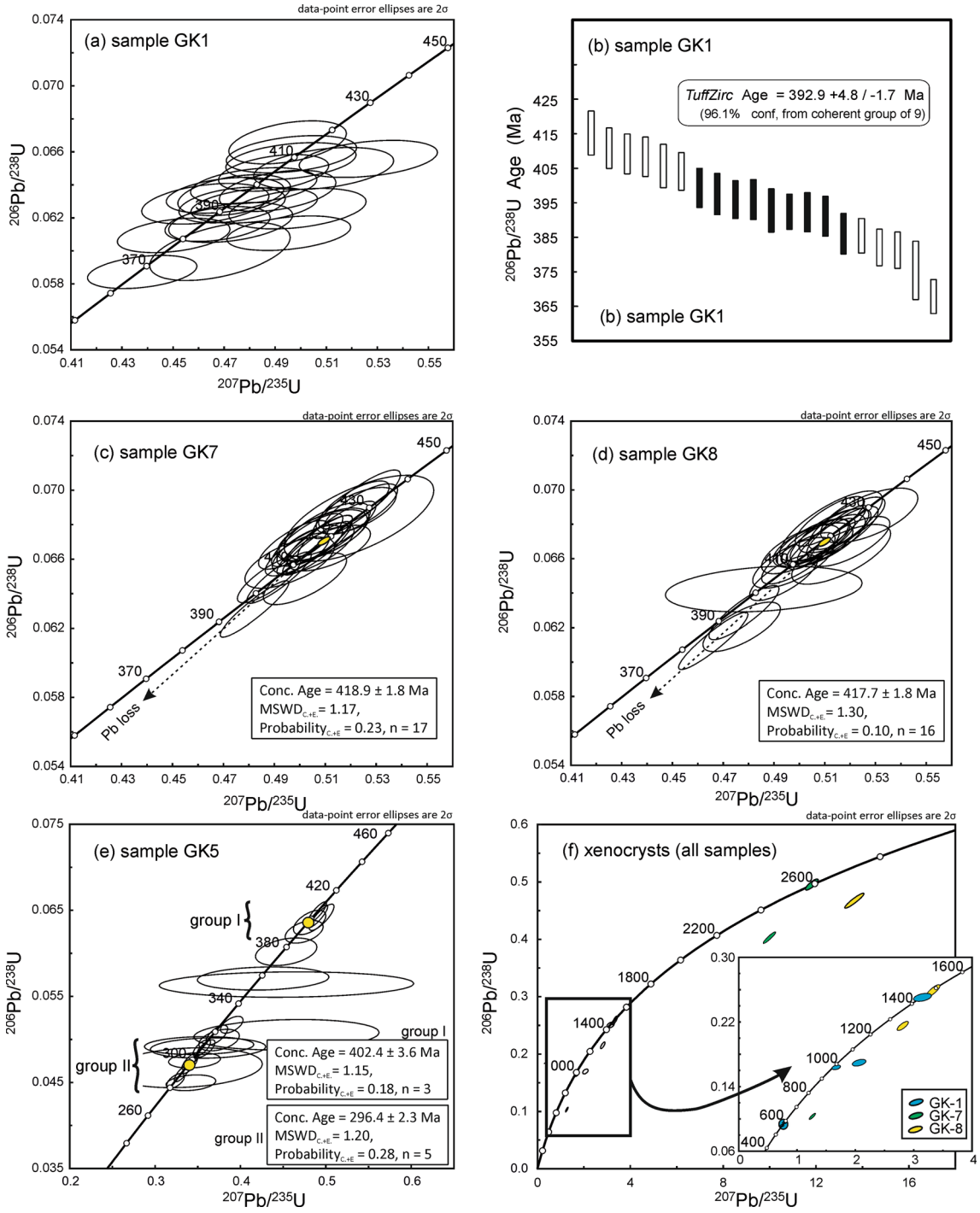

Fig. 8 Results of U–Pb dating of zircon from granite xenoliths of the Bode dike represented in Wetherill diagrams (**a**, **c**-**f**)—MSWD—Mean squared weighted deviation, c. + e.—of concordance and equivalence (for details see text)

Implications for Rheic Ocean closure

The Early Devonian intrusion ages (419–392 Ma) obtained from granitoid xenoliths of the Bodegang dike overlap geochronological data of felsic igneous rocks from the adjacent Mid-German Crystalline Zone, and Northern Phyllite Zone. Our ages are only slightly younger than emplacement ages of 444–423 Ma obtained from orthogneisses of the Ruhla Formation of the Mid-German Crystalline Zone (Brätz 2000; Zeh and Will 2010), which emplaced metasedimentary rocks of Paleozoic age (maximum depositional age at < 435 Ma; Zeh and Gerdes 2010), and from the drill core Saar

Table 1 Summary of rock types, zircon ages and Hf isotope compositions

Sample	Rock	Texture	AGE[a] (Ma)	± 2σ	$MSWD_{CE}$	$Prob_{CE}$	n	n[b] (All)	n[c] (Xeno)	$^{176}Hf/^{177}Hf_t$	± 2σ	εHf_t	± 2σ	*n*	Interpretation
GK1	Granitoid	Granular	392.9*	.+4.8/– 1.7			9	25	5	Not analysed					Emplacement age
GK2	Granite	Granophyric	Age reset at < 260 Ma					5		Not analysed					
GK5	Granite	Granophyric													
Group I			402.4	3.6	1.15	0.18	3	23		0.282439	0.000043	– 3.3	1.4	4	Reworked basement
Group II			296.4	2.3	1.20	0.28	5	23		0.282454	0.000031	– 5.0	1.2	5	Crystallisation age
GK7	Granitoid	Gneissic	418.9	1.8	1.17	0.23	17	27	3	0.282455	0.000067	– 2.4	2.7	6	Emplacement age
GK8	Granitoid	Gneissic	417.7	1.8	1.30	0.10	16	25	3	0.282448	0.000017	– 2.7	0.8	6	Emplacement age

a—concordia age, *weighted "Tuff zircon AGE"

b—number of all grains analysed per sample

c—number of xenocryst zircon (> 500 Ma)

$MSWD_{CE}$ Mean Square Weighted Deviation (of concordance and equivalence)

$Prob_{CE}$ Probability (of concordance and equivalence)

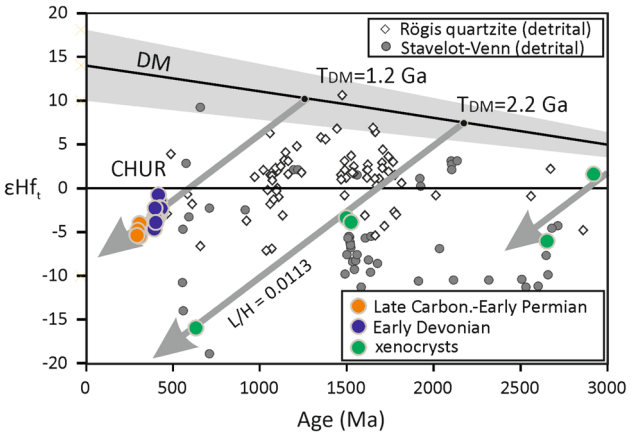

Fig. 9 Age versus εHf_t diagram showing the results of Lu–Hf isotope analyses of zircon grains from Bode dike xenoliths (red, blue, green circles). Data from the Stavelot–Venn Massif (Willner et al. 2013) and the Ruhla Crystalline Complex (Rögis quartzite: Zeh and Gerdes 2010) are shown for comparison. CHUR- chondritic uniform reservoir, DM- depleted mantle evolution, $L/H = {}^{176}Lu/{}^{177}Hf = 0.0113$, grey arrow—crust evolutionary trend. T_{DM}-two-stage Hf model age

1 (Sommermann and Satir 1993). In the Saar 1 drill core, the granite gneisses are overlain by a succession of middle to upper Devonian marine sediments deposited after 380 Ma (Zimmerle et al. 1976), indicating that the Late Silurian–Early Devonian magmatic arc was subsided beneath sea level during the opening of the Rhenohercynian Basin. Overlapping intrusion ages of 413–398 Ma were obtained from several other units of the Mid-German Crystalline Zone, e.g. Central Gneiss Unit of the Ruhla Crystalline Complex (Brätz 2000), Rotgneisses of the Spessart Crystalline Complex (Dombrowski et al. 1995), the eastern Odenwald (Reischmann et al. 2001) and the western Odenwald crystalline complexes (Dörr and Stein 2019). In the western Odenwald Silurian/Devonian granitoids locally intruded granitoids of Cadomian age (566 Ma) as has been shown by Dörr and Stein (2019). Volcanic counterparts of the Silurian–Devonian plutonic rocks, i.e. andesites and rhyolites with an age of ca. 433 Ma have also been described from the Northern Phyllite Zone by Sommermann et al. (1994).

Isotope–geochemical data reveal that most of the Silurian/Devonian granitoids and felsic volcanics of the Mid-German Crystalline Zone and Northern Phyllite Zone are calc-alkaline, and show typical magmatic arc signatures. Neodym-Sr isotope data further indicate reworking of older crust during granite emplacement (Dombrowski et al. 1995; Brätz 2000). These features are identical to those derived from the Bode dike xenoliths during this study, and suggest that granitoids beneath the eastern Harz Mountains and in the adjacent rock units formed part of a coherent Silurian–Devonian magmatic arc system (for compilations see Franke 2000; Zeh and Will 2010; Dörr and Stein 2019). Hafnium model

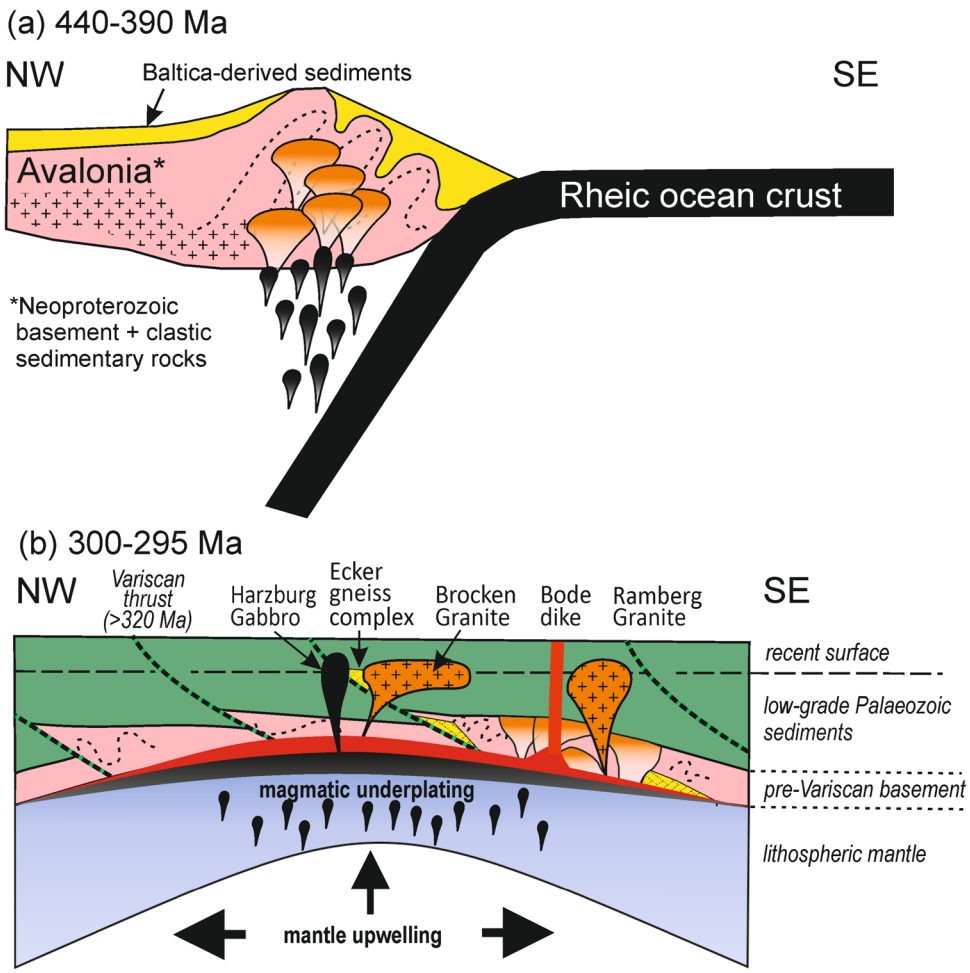

Fig. 10 Model explaining the formation of the granites found in xenoliths of the Bode dike of the eastern Harz Mountains. **a** Late Silurian to Early Devonian granite emplacement in a magmatic arc system caused by NW-ward subduction of the Rheic Ocean beneath Avalonia already attached to Baltica. **b** Partial melting of pre-Variscan basement beneath the Harz mountains caused by magmatic underplating during Late Carboniferous to Early Permian extension

ages of ca. 1.2 Ga derived from the Bode dike xenoliths are very likely meaningless in a geological context, and rather reflect mixing of mantle melts with crustal matter, comprising pre-Silurian igneous and metasedimentary rocks. This is directly indicated by zircon xenocrysts with Archean to Proterozoic ages found in several Bode dike xenoliths. The source of the zircon xenocrysts is ambiguous. Based on their ages, these could result from the reworking of Cadomian orthogneisses (as described from the Odenwald by Dörr and Stein 2019), but also from (meta)sedimentary rocks deposited at < 565 Ma ($^{206}Pb/^{238}U$ age of the youngest xenocryst in sample GK1). We note that detrital zircon grains with ages of 580 ± 20 Ma are extremely rare (< 2%) in quartzites of presumed Silurian–Devonian protolith age, as exposed in the Ecker Gneiss complex of the Harz Mountains (Geisler et al. 2005; Linnemann et al. 2023), in the Rhenish Massif (Eckelmann et al. 2014), and in the Ruhla Formation of the Mid-German Crystalline Zone (Zeh and Gerdes 2010). However, such grains occur relatively abundant (ca. 20%) in metagreywackes of presumed Neoproterozoic age of the Northern Phyllite Zone (Warstein paragneiss; Dörr and Stein 2019), and in lower Cambrian to Silurian sediments of the Brabant Massif (Linnemann et al. 2012; Willner et al. 2013), having an Avalonia provenance. Thus, the finding of xenocrysts with ages of 570–600 Ma, c. 1.5 Ga and 2.6–2.9 Ga in the Bode dike xenoliths points to the assimilation of Avalonia-derived sediments, which is also supported by overlap in age-Hf isotope data (Fig. 9). We further note that Hf model ages of ca. 1.2 Ga derived from zircon grains in the Bode dike xenoliths overlap well with Nd model ages of 1.03–1.34 Ga estimated for Silurian intrusive and volcanic rocks of the Brabant Massif (Linnemann et al. 2012).

In summary, comparison of zircon age-Hf data and whole-rock isotope–geochemical results suggests that Silurian to early Devonian granitoid rocks constituting the basement beneath the eastern Harz Mountains formed part of a magmatic arc system, which resulted from westward subduction of the Rheic Ocean beneath Avalonia, which at 420–395 Ma was already connected to Baltica (see model in Zeh and Gerdes 2010; Linnemann et al. 2023), and overlain by Baltica-derived clastic sedimentary rocks (Fig. 10a).

During Variscan collision at < 330 Ma, the Rheic Ocean and the Rhenohercynian "back arc" basin became finally closed (see model in Zeh and Gerdes 2010), and the

Silurian–Devonian magmatic arc fragmented and overthrust by very low-grade metasedimentary rocks of Paleozoic age (mostly Emsian to Visean), resulting in the NW-vergent fold-and-thrust architecture of the Harz Mountains. As shown by Franke (2000) and Linnemann et al. (2023), the Paleozoic sedimentary units of the Harz Mountains were supplied from very different sources: from Baltica-Avalonia, from Cadomia, and the Late Devonian–Carboniferous flysch from the Mid-German Crystalline Zone. Finally, all rock units became juxtaposed in a giant accretionary prism and were affected by very low-grade metamorphic overprint. The only exceptions are exotic slivers of Variscan high-grade paragneiss with Baltica affinity, the so-called Ecker Gneisses (Fig. 10b). It is likely that the Devonian granites, exposed as xenoliths in the Bode dike, were also deformed during Variscan collision, although there is no direct evidence for it.

Conclusions

1. The Bode dike of the eastern Harz Mountains contains xenoliths of granite composition, in addition to metasedimentary rocks and amphibolites.
2. The granite protoliths were formed during two different magmatic events, as indicated by combined results of petrography, zircon U–Pb dating, Hf isotope analyses and whole-rock geochemistry.
3. Deformed granites are witnesses for the existence of a Late Silurian–Early Devonian magmatic arc system, which resulted from NW-ward subduction of the Rheic Ocean beneath Avalonia-Baltica between 440 and 390 Ma.
4. Granites with granophyric textures result from remelting of Silurian–Devonian granites, due to mantle upwelling in an extensional regime, which affected wide parts of Central Europe during the Late Carboniferous–Early Permian.

Supplementary Information The online version contains supplementary material available at https://doi.org/10.1007/s00531-024-02429-3.

Acknowledgements AZ is grateful to Axel Gerdes and Linda Markow (FIERCE Frankfurt) for help with Lu-Hf isotope analyses and Deutsche Forschungsgemeinschaft (DFG) for financial support (grant ZE424/17-1). We also thank Marion Tichomirowa (TU Freiberg) for providing REM zircon images, as well as Milan Kohùt and an anonymous reviewer for helpful comments on a former version of the manuscript, and Ulrich Riller for editorial handling.

Author contribution Armin Zeh: conceptualization, U–Pb dating, Hf isotope analyses, trace element analyses formal analysis, investigation, writing—original draft, funding acquisition. Carl-Heiz Friedel: sampling, petrography, writing, editing. Olaf Tietz: sampling, writing—review and editing. István Dunkl: U–Pb dating, writing. All authors read and approved the final manuscript.

Funding Open Access funding enabled and organized by Projekt DEAL.

Data availability The dataset generated and analyzed during the current study are available from the corresponding author on request.

Declarations

Conflict of interest The authors declare that they have no known competing financial interests or personal relationships that could have appeared to influence the work reported in this paper.

References

Appel P, Stipp M, Friedel C-H, Fiedrich A, Krauss K, Berger S (2019) U-Th-total Pb ages of monazite from the Eckergneiss (Harz Mountains, Germany): evidence for Namurian to Westfalian granulite facies metamorphism at the margin of Laurussia. Int J Earth Sci 108:1741–1753

Baumann A, Grauert B, Mecklenburg S, Vinx R (1991) Isotopic age determinations of crystalline rocks of the Upper Harz Mountains. Germany Geol Rundsch 80(3):669–690

Bouvier A, Vervoort JD, Patchett PJ (2008) The Lu-Hf and Sm-Nd isotopic composition of CHUR: constraints from unequilibrated chondrites and implications for the bulk composition of terrestrial planets. Earth Planet Sci Lett 273:48–57

Brätz H (2000) Radiometrische Altersdatierungen und geochemischen Untersuchungen von Orthogneisen, Granite und Granitporphyren aus dem Ruhlaer Kristallin, Mitteldeutsche Kristallinzone. Dissertation Univ. Würzburg, Germany: pp 1–151

Chappell BW, White AJR (1974) Two contrasting granite types. Pac Geol 8:173–174

Chauvel C, Blichert-Toft J (2001) A hafnium isotope and trace element perspective on melting of the depleted mantle. Earth Planet Sci Lett 190:137–151

Couzinié S, Laurent O, Moyen J-F, Zeh A, Bouilhol P, Villaros A (2016) Post-collisional magmatism: crustal growth not identified by zircon Hf-O isotopes. Earth Planet Sci Lett 456:182–195

Dombrowski A, Henjes-Kunst F, Höhndorf A, Kröner A, Okrusch M, Richter P (1995) Orthogneisses in the Spessart Crystalline Complex, Northwest Bavaria: Witnesses of Silurian granitoid magmatism at an active continental margin. Geol Rund 84:399–411

Dörr W, Stein E (2019) Precambrian basement in the Rheic suture zone of the Central European Variscides (Odenwald). Int J Earth Sci 108:1937–1957

Dunkl I, Mikes T, Simon K, von Eynatten H (2008) Brief introduction to the Windows program Pepita: data visualization, and reduction, outlier rejection, calculation of trace element ratios and concentrations from LA-ICP-MS data. In: Laser ablation ICP-MS in the Earth Sciences. In: Sylvester P (eds) Current practices and outstanding issues. Mineralogical Association of Canada, Short Course 40: 334–340

Eckelmann K, Nesbor H, Königshof P, Linnemann U, Hofmann M, Lange J-M, Sagawe A (2014) Plate interactions of Laurussia and Gondwana during the formation of Pangaea – constraints from U-Pb LA–SF–ICP–MS detrital zircon ages of Devonian and Early Carboniferous siliciclastics of the Rhenohercynian zone, Central European Variscides. Gondwana Res 25:1484–1500

Franke W (2000) The mid-Europian segment of the Variscides: tectonostratigraphic units, terrane boundaries and plate tectonic evolution. In: Franke W, Haak V, Oncken O, Tanner D (eds) Orogenic processes: quantification and modelling in the Variscan Belt. Geol Soc London Spec Publ 179: 35–62

Frost BR, Frost CD (2008) A geochemical classification for feldspathic igneous rocks. J Petrol 49:1955–1969

Frost BR, Barnes CG, Collins WJ, Arculus RJ, Ellis DJ, Frost CD (2001) A geochemical classification for granitic rocks. J Petrol 42:2033–2048

Geisler T, Vinx R, Martin-Gombojav N (2005) Pidgeon RT (2005) Ion microprobe (SHRIMP) dating of detrital zircon grains from quartzites of the Eckergneiss Complex, Harz Mountains (Germany): implications for the provenance and the geological history. Int J Earth Sci (geol Rundsch) 94:369–384

Gerdes A, Zeh A (2006) Combined U-Pb and Hf isotope LA-(MC-) ICP-MS analyses of detrital zircons: Comparison with SHRIMP and new constraints for the provenance and age of an Armorican metasediment in Central Germany. Earth Planet Sci Lett 249:47–61

Gerdes A, Zeh A (2009) Zircon formation versus zircon alteration – new insights from combined U-Pb and Lu-Hf in-situ LA-ICP-MS analyses, and consequences for the interpretation of Archean zircon from the Limpopo Belt. Chem Geol 261:230–243

Goll M, Lippolt HJ, Obert C, Schwarz W (1998) Datierungen zum permokarbonen Magmatismus des Harzes - erste K-Ar-Ergebnisse. Terra Nostra 98(2):62–65

Harrison TM, Watson EB (1983) Kinetics of zircon dissolution and zirconium diffusion in granitic melts of variable water content. Contrib Miner Petrol 84:66–72

Huckriede H, Wemmer K, Ahrendt H (2004) Palaeogeography and tectonic structure of allochthonous units in the German part of the Rheno-Hercynian Belt (Central European Variscides). Int J Earth Sci (geol Rdsch) 93:414–431

Kossmat F (1927) Gliederung des varistischen Gebirgsbaues. Abh d Sächs Geol Landesamts 1:1–39

Laurent O, Zeh A (2015) A simple Hf isotope-age array despite different granitoid sources and complex Archean geodynamics: an example from the Pietersburg block (South Africa). Earth Planet Sci Lett 430:326–338

Linnemann U, Herbosch A, Liégeois J-P, Pin C, Gärtner A, Hofmann M (2012) The Cambrian to Devonian odyssey of the Brabant Massif within Avalonia: a review with new zircon ages, geochemistry, Sm–Nd isotopes, stratigraphy and palaeogeography. Earth Sci Rev 112:126–154

Linnemann U, Zweig M, Zieger-Hofmann M, Vietor T, Zieger J, Haschke J, Gärtner A, Mende K, Krause R, Knolle F (2023) The Harz Mountains (Germany) – Cadomia meets Avalonia and Baltica: U-Pb ages of detrital and magmatic zircon as a key for the decoding of Pangea's central suture. Geol Soc London, Spec Publ 542, in press. https://doi.org/10.1144/SP542-2023-52

Lippolt H, Hess J (1996) Numerical stratigraphy of Permocarboniferous volcanic rocks from Central Europe. Part II: Western Harz. Zeitschr Deutsch Geol Gesellschaft 147:1–9

Ludwig KR, Mundil R (2002) Extracting reliable U-Pb ages and errors from complex populations of zircons from Phanerozoic tuffs. Geochim Cosmochim Acta 66(Suppl. 1):461

Ludwig KR (2012) User's manual for Isoplot 3.75: A geochronological Toolkit for Microsoft Excel. Berkeley Geochronology Center Special Pub 4: pp 70

Lützner H, Tichomirowa M, Käßner A, Gaupp R (2021) Latest Carboniferous to early Permian volcano-stratigraphic evolution in Central Europe: U-Pb CA–ID–TIMS ages of volcanic rocks in the Thuringian Forest Basin (Germany). Int J Earth Sci 110:377–398

Maniar PD, Piccoli PM (1989) Tectonic discrimination of granitoids. Bull Geol Soc America 101:635–643

McCann T, Pascal C, Timmerman MJ, Krzywiec P, López-Gómez J, Wetzel L, Krawczyk CM, Rieke H, Lamarche J (2006) Post-Variscan (end Carboniferous-Early Permian) basin evolution in Western and Central Europe. Geol Soc London Mem 32:355–388

McDonough WF, Sun S-S (1995) Composition of the Earth. Chem Geol 120:223–253

Obst K, Katzung G, Haupt U (2001) Dyke magmatism in the central Harz mountains and its implication for Late Variscan extensional tectonics. N Jb Geol Paläont Abh 219(3):393–432

Pearce JA, Harris NBW, Tindle AG (1984) Trace element discrimination diagrams for the tectonic interpretation of granitic rocks. J Petrol 25:956–983

Pupin JP (1980) Zircon and granite petrology. Contrib Mineral Petrol 73:207–220

Reischmann T, Anthes G, Jaekel P, Altenberger U (2001) Age and origin of the Böllsteiner Odenwald. Min Petrol 72:29–44

Scherer E, Münker C, Mezger K (2001) Calibration of the lutetium-hafnium clock. Science 293:683–687

Schust F (1958) Über das Verhältnis des Bodeganges zum Ramberggranit. Ber Geol Ges DDR 3:75–79

Schwab M (2008) Harz. In: Bachmann GH, Ehling BC, Eichner R, Schwab M (eds) Geologie von Sachsen-Anhalt. Schweizerbart, Stuttgart, pp 408–457

Schwab M, Ehling B-C (2008) Karbon. In: Eichner R, Schwab M (eds) Bachmann GH, EhlingB-C. Geologie von Sachsen Anhalt. Schweitzerbart, Stuttgart, pp 110–140

Schwab M, Hüneke H (2008) Devon. In: Bachmann GH, Ehling B-C, Eichner R, Schwab M (eds) Geologie von Sachsen Anhalt. Schweitzerbart, Stuttgart, pp 87–109

Söderlund U, Patchett PJ, Vervoort JD, Isachsen CE (2004) The 176Lu decay constant determined by Lu-Hf and U-Pb isotope systematics of Precambrian mafic intrusions. Earth Planet Sci Lett 219:311–324

Sommermann AE, Satir M (1993) Zirkonalter aus dem Granit der Bohrung Saar I. Beih Eur J Mineral 5(1):145

Sommermann A-E, Anderle H-J, Todt W (1994) Das Alter des Quarzkeratophyrs der Krausaue bei Rüdesheim am Rhein (Blatt 6013 Bingen, Rheinisches Schiefergebirge). Geol Jahrb Hessen 122:143–157

Stacey JS, Kramers JD (1975) Approximation of terrestrial lead isotope evolution by a two-stage model. Earth Planet Sci Lett 26:207–221

Taylor SR, McLennan SM (1985) The continental crust: its composition and evolution. Blackwell, Oxford: pp 312

Tietz O (1996) Zur Geologie, Geochemie, Zirkon- und Xenolithführung des Bodeganges an den Gewitterklippen bei Thale (Harz), sowie vergleichende Untersuchungen zur Zirkontypologie benachbarter permosilesischer Magmatite. Abh Ber Naturkundemus Görlitz 69(4):1–100

Tietz O (1995) Zur Geologie des Bodeganges an den Gewitterklippen bei Thale/Harz. In: Schwab M (eds) 9. Rundgespräch Geodynamik

des europäischen Variszikums. Zbl Geol Paläont, Teil 1, 1993: 1574–1576
Van Achterbergh E, Ryan CG, Griffin WL (2000) GLITTER: On-Line Interactive Data Reduction for the Laser Ablation ICP-MS Microprobe. Macquarie University: pp 61
Van Wees J-D, Stephenson RA, Ziegler PA, Bayer U, McCann T, Dadlez R, Gaupp R, Narkiewicz M, Bitzer F, Scheck M (2000) On the origin of the Southern Permian Basin, Central Europe. Mar Petrol Geol 17:43–59
Von Seckendorff V (2012) Der Magmatismus in und zwischen den spätvariszischen permokarbonen Sedimentbecken in Deutschland. Schriftr Deutsch Gesellschaft Geowiss 61:743–860
Wachendorf H, Buchholz P, Zellmer H (1995) Fakten zum Harz-Paläozoikum und ihre geodynamische Interpretation. Nova Acta Leopoldina NF 71(291):119–150
Wedepohl KH (1995) The composition of the continental crust. Geochim Cosmochim Acta 59:1217–1232
Willner AP, Barr SM, Gerdes G, Massonne HJ, White CE (2013) Origin and evolution of Avalonia: evidence from U-Pb and Lu– Hf isotopes in zircon from the Mira terrane, Canada, and the Stavelot-Venn Massif, Belgium. J Geol Soc Lond 170:769–784
Wilson M, Neumann E-R, Davies GR, Timmermann MJ, Heeremans M, Lasen BT (2004) Permo-Carboniferous magmatism and rifting in Europe. Geol Soc London Spec Publ 223:498
Woodhead JD, Hergt JM (2005) A Preliminary Appraisal of Seven Natural Zircon Reference Materials for In Situ Hf Isotope Determination. Geostand Geoanalytical Res 29:183–195
Zech J, Jeffries T, Faust D, Ullrich B, Linnemann U (2010) U/Pb-dating and geochemical characterization of the Brocken and the Ramberg Pluton. Pluton, Harz Mountains, Germany, Geologica Saxonica 56(1):9–24
Zeh A, Brätz H (2000) Radiometrische und morphologische Untersuchungen an Zirkonen aus Granitporphyren, Rhyolithen und Granitgeröllen des nordwestlichen Thüringer Waldes. Z Dt Geol Ges 151:187–206
Zeh A, Gerdes A (2010) Baltica- and Gondwana-derived sediments in the Mid-German Crystalline Rise (Central Europe): Implications for the closure of the Rheic ocean. Gondwana Res 17:254–263
Zeh A, Gerdes A (2012) U-Pb and Hf isotope record of detrital zircons from gold-bearing sediments of the Pietersburg Greenstone Belt (South Africa) – Is there a common provenance with the Witwatersrand Basin? Precam Res 204–205:46–56
Zeh A, Will TM (2010) The Mid-German Crystalline Zone. In: Linnemann U, Romer R (eds) Pre-Mesozoic Geology of Saxo-Thuringia – From the Cadomian Active Margin to the Variscan Orogen. Schweizerbart, Stuttgart, pp 195–220
Zeh A, Cosca MA, Brätz H, Okrusch M, Tichomirowa M (2000) Simultaneous horst-basin formation and magmatism during Late Variscan transtension: evidence from 40Ar/39Ar and 207Pb/206Pb geochronology in the Ruhla Crystalline Complex. Int J Earth Sci 89:52–71
Ziegler PA (1990) Geological atlas of western and Central Europe 1990. Blackwell, Oxford: pp 239
Zimmerle W, Hering O, Ghazanfari A, Weber G, Krebs C, Tan CL, Nickel E, Reible P (1976) Die Tiefbohrung Saar 1.-Petrographische Beschreibung und Deutung der erbohrten Schichten. Geol Jb, Reihe A 27:91–305